RSC Advances

ROYAL SOCIETY OF CHEMISTRY

www.rsc.org/advances

RSC Advances

PAPER

Biocompatible and Biodegradable elastomer/fibrinogen composite electrospun scaffolds for cardiac tissue regeneration

Received 01st October 2015,
Accepted 00th October 2015

DOI: 10.1039/x0xx00000x

www.rsc.org/RSC Advances

MerumSireesha[a], Veluru Jagadeesh Babu[b]*, Seeram Ramakrishna [a,c]*

In this study, a mixture of elastomeric polymer poly [1,8-octanediol-co-(citric acid) -co- (sebacic acid)] or POCS and figbrinogen (FBN) were employed to prepare electrospun nanofibrous scaffolds. POCS and FBN concentrations were varied POCS:FBN:0:100 as a control, POCS:FBN:25:75 and POCS:FBN:50:50. All the scaffolds were characterized by contact angle measurments, scanning electron microscopy (SEM), FTIR, mechanical test and cell proliferation studies. The contact angle measurements confirmed that POCS:FBN:50:50 scaffolds were hydrophilic. While the scaffold diameters were confirmed with SEM were in the range of 440 ± 120 nm.From the FT-IR,the high intense peak was observed at 1738 cm^{-1} for Scaffold POCS:FBN:25:75 and POCS:FBN:50:50 which is attributed to –C=O vibrations of ester absorption and confirms the presence of polyester. The Young's modulusfor POCS:FBN:50:50 scaffold was evolved as 0.27± 0.07 MPa and compared with native human myocardium. Furthermore the scaffolds were carried for cell proliferation studiesby means of MTS [3-(4,5-dimethylthiazol-2-yl)-5-(3-carboxymethoxyphenyl)-2-(4- sulfophenyl)-2H-tetrazolium, inner salt] assay. Human cardiomyocytes (HCMs) were seeded on the scaffolds and the interaction of cell-scaffold constructs were evaluated. Proliferation of cardiomyocytes (CMs) on scaffold was observed and presented. The interactions between cells and substrate were analyzed by using confocal microscopy. The electrospun composite scaffolds of POCS/FBN proved to yield flexibility and biodegradability. From the in-vitro biocompatability studies, we anticipate that the scaffold POCS:FBN:50:50 would be potential for cardiac tissue regeneration.

1. Introduction:

In general, tissue engineering is an multi-disciplinary area that aim to replace or regenerate a new tissue where it necessary[1]. Fibrinogen (FBN) is one of the naturally occurring glycoprotein that extensively used in tissue engineering [2, 3]. The degradation products of FBN exhibit distinctive properties such as improved healing mechanism (in-vitro and in-vivo), protective against myocardial reperfusion injury, easily degradable, non-immunogenic and promote increased cell migration[4-6]. However, pure FBN scaffolds doesn't show enough mechanical integrity to assist on its own to sustain a longer period of time. Therefore, the biocompatible and biodegradable scaffold which can fulfil and retrieve from multiple deformation without troubling the surrounding healthy tissue would be more beneficial[7]. In addition, elasticity is also a major concern in cardiac tissues. Therefore, intense research efforts focused on preparation of innovative bio-elastomers for the development of soft tissue regeneration and mimicking the native tissue[8]. Djordjevic*et.al.,* synthesized an elastomeric polymer and tested to mimic the extra cellular matrix (ECM)[9, 10]. These elastomeric polymers with additional mechanical integrity can promote healthy tissue formation [11, 12]. The obtained elastomeric POCS or poly [1,8-octanediol-co-(citric acid) -co- (sebacic acid)] was synthesized by a simple polyesterification of 1,8-octanediol (OD), citric acid (CA) and sebacic acid (SA)[7, 13]. POCS showed high degree of elasticity for the regeneration of soft tissues. The main virtue of this elastomers is to improve the elasticity and develop the ability to withstand strong deformation forces (restore the original shape and size upon removal of stress)[14]. Therefore, the blend of POCS elastomer and FBN based scaffolds would expected to be biodegradable, non-immunogenic and promote improved cell migration.

While the electrospun nanostructures[15] were explored in tissue engineering[16], the improved specific surface area can provide more adherence site to cell membrane receptors, unlike micro-scale and flat surfaces[17]. Sell *et.al.,* reported that the use of natural polymers based electrospun nanofibers in creation of bioactive ECM analogues in tissue engineering[18]. Mc Manus et.al, synthesized the FBN based electrospun nanofibrous scaffolds in support of tissue growth technologies [19]. He et.al., reported the FBN based nanofibrous scaffolds for

[a]*Center for Nanofibers and Nanotechnology, Nanoscience and Nanotechnology Initiative, Faculty of Engineering , National University of Singapore, Singapore.*
Email: seeram@nus.edu.sg
[b]*Department of Chemical and Biomolecular Engineering, National University of Singapore, 4 Engineering Drive 4, Singapore 117 585, Singapore.*
Email: vjbabu2002@gmail.com ; or chejbv@nus.edu.sg ;
[c]*Department of Mechanical Engineering, National University of Singapore, 2 Engineering Drive 3, Singapore-117576, Singapore.*

in-vitro attachment of mouse fibroblasts (L929 cells) for soft tissue concentrations[20], and spreading microfilament organization of human endothelial cells[21]. The interactions between the cell-scaffold construct would enhance the survival of cardiomyocytes[22].

In this study, we postulated the POCS/FBN for the reparation of composite scaffolds at different ratios *viz,* POCS:FBN:0:100 (scaffold S1) as a control, POCS:FBN:25:75 (scaffold S2) and POCS:FBN:50:50 (scaffold S3). We employed electrospinning to synthesize nanofibrous scaffolds, these scaffolds were characterized by contact angle measurements, morphological, chemical and mechanical properties. The composite scaffolds were seeded with human cardio myocytes (HCMs) and examined for the cell-specific interaction to analyse the biocompatibility of the scaffolds for myocardial tissue engineering. These composite scaffolds are expected to provide more support to the HCMs than pure FBN and/or POCS scaffolds. Over and above, these composite scaffolds are hypothetically enhance the cell adherence. From these investigations, the scaffold S3 performance showed the promising for the tissue regeneration.

2. Materials and methods

2.1. Materials

Citric Acid (CA; 99.5%, ACS reagent) and 1,8-Octanediol (98%) were purchased from Sigma-Aldrich (Steinheim, Germany). Fibrinogen (FBN), 1,1,1,3,3,3-hexafluoro-2-propanol (HFP), Hexamethyldisilazane (HMDS), Bovine serum albumin(BSA), and ethanol were purchased from Sigma Aldrich (St. Louis, USA). Monoclonal anti-Troponin-I and anti-Myosin Heavy Chain antibody were purchased from Abcam (singapore). Human cardiomyocytes (HCMs), Myocyte growth media and Dulbecco's Modified Eagle's media (DMEM) were purchased from Promocell (Singapore). Phosphate buffered saline (PBS), Fetal Bovine Serum (FBS), antibiotics and trypsin-ethylenediamine tetra acetic acid (EDTA) were purchased from Gibco, Invitrogen Corp, USA. Cell titre 96 aqueous one solution was purchased from Promega (WI, USA) and polyvinyl alcohol mounting medium were obtained from Fluka, Singapore.

2.2. Methods:

POCS elastomer synthesis:

The synthesis of poly [1,8-octanediol -co- (citric acid) -co- (sebacic acid)] or POCS was synthesized according to the previous reports[16, 23], as briefly: equimolar ratios of 1,8-Octonediol and acids (CA and SA) in 1:1 were mixed together in a round bottom flask at 160 °C in presence of oil bath under magnetic stirrer. The flask was kept in an inert atmosphere of nitrogen for approximately 30 min. Since, the monomer CA would react with diol *via* polycondensation reaction and results in cross-linking of polymers. Then the temperature of the flask was lowered down to 140 °C and it was continued for 1 hr. for further increase in the degree of cross-linking and elasticity. The chemical structures of the elastomer polymer are presented in Figure 1(a).

Electrospun Scaffold Fabrication

The FBN nanofibers were prepared by taking 12 % (w/v) of FBN in 1 mL of HFP solution and carried out for electrospinning with home-made set-up. The electrospinning process is similar to our earlier reports [24, 25]. Approximately, 3 mL of solution was loaded in syringe and connected with 18G needle. The solution was fixed to feed at a rate of 0.80 mL/h using a syringe pump (KD scientific, Holliston, USA) and the distance between needle and the substrate was maintained at 8 cm apart. The optimal DC voltage 18kV was set to obtain uniform nanofibers and were collected on 15 mm glass coverslips. For producing POCS/FBN composite fibers, the similar conditions were maintained (except the needle 27G1/4). Initially, POCS dissolved in 1 mL of HFP and then added with FBN. POCS concentrations was varied as 25, 50 % (w/w %) in FBN. All the electrospun nanofibers were subsequently vacuum dried to remove any residual solvent present in the fibers. These POCS:FBN:0:100; POCS:FBN:25:75 and POCS:FBN:50:50 nanofibers named as Scaffold S1, scaffold S2 and Scaffold S3 respectively. POCS:FBN:100:0 (pure POCS) nanofibers were tried to prepare, but due to high viscosity could not possible to spin *via* electrospinning.

FBN Cross-linking

Pure FBN scaffolds were cross-linked with glutaraldehyde vapors to improve their structural and mechanical properties. The electrospun nanofibers were placed under 50%of glutaraldehyde vapors at room temperature in a tightly closed container. The time allowed for cross-linking was about 30 min and then vacuum dried for about 15-20 min.

2.3. Characterization:

Water contact angle of all the scaffolds S1, S2 and S3 were measured using a VCA Optima XE video contact angle system (Crest Technology, Singapore) mounted with a CCD camera. Scanning electron microscopy (SEM) images (JSM5600, JEOL, Japan) were obtained at an accelerating voltage of 10 kV, for better resolution approximately 5 nm of gold was sputtered on the fibers using JEOL JFC-1200 Auto Fine Coater, Japan. The electrospun scaffolds were soaked into PBS (pH of 7.4) over a period of 30 days at about 37 °C for checking the biodegradation property, then observed in SEM. After 5 days of PBS degradation the scaffolds were washed and subsequently vacuum died. These PBS degraded and pure samples were carried for Fourier transform infrared (FTIR) spectroscopic analysis at a resolution rate of 3 cm^{-1} within the range of 500 to 4000 cm^{-1} by using Avatar 380 FTIR spectrometer (Thermo Nicolet, Waltham, MA). Instron3345 table top tensile tester (MA, USA) was used to study the tensile test. A load cell capacity of 10N and crosshead speed of 5 mm/min under ambient conditions. This experiment was

repeated at least five times and the best results were plotted on stress-strain curves for obtaining Young's modulus.

Biocompatibility and Cell proliferation studies

HCMs were cultured in myocyte growth media (10% of FBS and 1% of antibiotics i.e. penicillin 100 units per mL and streptomycin 100 µg/ mL). The tissue culture incubators were set at 37 °C for 5% CO_2. The cell culture media was changed at every alternate days. After reaching cell confluence of about 80-90%, they were trypsinized (1xTrypsin) and centrifuged. The extracted myocytes are seeded onto the electrospun scaffolds collected on 15 mm diameter glass cover slips. Before seeding, scaffolds were placed in a 24-well plate with a stainless steel ring and sterilized for 2 hr. under ultraviolet (UV) light. After sterilization, the scaffolds were treated thrice with PBS at an interval of 15 min to remove any residual solvent and soaked in myocyte growth media for overnight to remove toxic substances. These scaffold constructs were treated with PBS and incubated with 3% glutaraldehyde solution for 3 hr. This was repeated by changing concentration levels of ethanol (50, 75, 90 and 100 %) and added with HMDS and then air dried. The cell proliferation on scaffolds was studied by MTS [3-(4,5-dimethylthiazol-2-yl)-5-(3-carboxymethoxyphenyl)-2-(4-sulfophenyl)-2H-tetrazolium, inner salt] assay calorimetric method and the efficacy was about $1x10^4$ cells/cm^2 over a period of six days. The media was removed and the cell-substrate was rinsed once with PBS. The scaffolds were, further added with 20% of the cell titre reagent with serum-free myocyte growth media, incubated for 3 hr. The absorbance was measured at 490 nm using a micro plate reader (FLUOstar OPTIMA; BMG Lab Technologies, Germany). HCMs were also seeded on control tissue culture plate (TCP) coverslips as a positive control.

Immunocytochemistry studies:

For evaluating the functional ability of the HCMs, immunocytochemical studies were performed. After seeding the cells on scaffolds, cardiomyocytes were stained with two different cardiac proteins, namely Troponin-I (Trp-I) and Myosin heavy chain (MHC). After four days of cell culture, the media was aspirated out and the scaffolds were rinsed in PBS, then formalin was added to fix the cells for about 20 min. The nonspecific sites were blocked for 90 min by using 3% of BSA. Trp-I and MHC were diluted in the ratios of 1:100, and stained for about 90 min. The cell-substrate samples were treated thrice with PBS and incubated with Alexa 488 goat anti-mouse IgG secondary antibody for 60-90min at room temperature. The nucleus of the cells was stained with 4', 6'-diamidino-2-phenylindole hydrochloride (DAPI). The cell-substrate were rinsed about 5 times with PBS to remove excess staining, the samples were air dried and mounted onto a glass slide using fluoromount and observed under laser scanning confocal microscope (LSCM, Fluoview FV300, Olympus).

2.4. Statistical Analysis:

Data were determined using one way analysis of variance (ANOVA) in which appropriate, Statistical significance was performed by using student's t-test at $p \leq 0.05$.

3. Results and Discussion:

The water contact angle for scaffold S1 is about 111.65 ± 8° which is hydrophobic. While the scaffold S2 and S3 are showed 48.81 ± 9 ° and 58.85 ± 10° are hydrophilic. Since the increased content of the POCS in FBN, the contact angle also increased and thus the nature of the scaffolds also changed from hydrophobic to hydrophilic. Hydrophilic surfaces of the biomaterial regulate cell attachment and proliferation. Arima and Iwata, reported that if the water contact angle is between 40 - 70°, the cells can effectively adhere onto polymer surfaces [26]. In the present studies, FBN shows the hydrophobic which comes from the thermodynamic state of the surface roughness [27]. It is not so surprising that the hydrophobic gradually converted to hydrophilic due to the FBN blended with the POCS which is with –COOH functional group. In addition, the fiber diameters can also be controlled by changing the concentration level of POCS [27]. The fiber morphology was observed by using SEM and presented in figure 1 (b-d) shows as-spun scaffolds are bead-free and continuous. The nanofiber diameters were evaluated by using UTHSCSA Image Tool 3.00 software and shown in Table 1. Chen et.al., reported that the fiber diameters 400 nm has significantly influence on cell attachment and growth [28] parameters. As presented in table-1, the decrease in fiber diameter with increased content of POCS in FBN could be advantage in tissue regeneration. The diameters of the scaffold S3 (POCS: FBN: 50:50) is in comparable range for tissue culture studies.

In order to check the degradation, all the scaffolds were soaked in PBS solution and the morphology was observed after 5, 10, 15 and 30. Figure 2 shows the SEM images of scaffolds after soaking in to PBS solution. The respective names and labels are given on SEM images (scaffolds S1 (a, b, c and d), S2 (e, f, g and h) and S3 (I, j, k and l) for 5, 10, 15 and 30 day respectively). From Figure 3 a, scaffold S1 shows the reasonable degradation on 5^{th} day. Whereas, for scaffold S2 does not show any degradation up to 15^{th} day but on 30^{th} day showed partial degradation. The scaffold S3 started to degrade from the day 15^{th} and complete degradation was observed on 30^{th} day. The degradation performance wise, the scaffold S3 is the superior than remaining scaffolds.

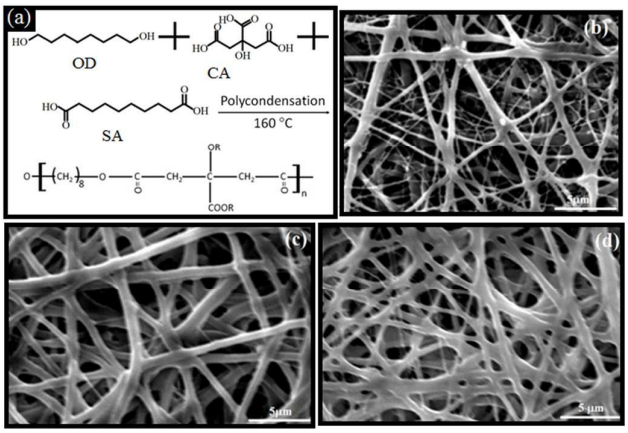

Figure 1: A schematic representation of (a) Chemical structures of the CA, POC and SA reproduced from Ref[10], (b) S1 (c) S2 and (d) S3 electrospun nanofibers morphology.

Figure 3, shows the FTIR spectra of scaffolds before and after soaking into PBS solution. The scaffold S1 shows the FTIR peak at 1655 and 1548 cm^{-1} are ascribed due to amide I and amide II bands respectively, which are very common for proteins with high α-helix content. These two bands are attributed due to C=O stretching type vibrations and in-plane N-H bending. Scaffold S2 shows peak at 1738 cm^{-1} are attributed –C=O vibrations of ester absorption and confirms the presence of polyester. The same peak was also observed in scaffold S3 with more intensity. While the peak at 2938 cm^{-1} is attributed to methylene group which is confirmed for the elastomer. The broadband centred at 3296 and 3490 cm^{-1} are assigned due to H-OH and H-COOH respectively [23]. As shown in Figure 3, the scaffolds even after PBS treatment, does not show any significant changes in FTIR peak positions and remains unchanged.

In order to identify the mechanical strength of the scaffolds, the stress-strain relationship was observed and presented in figure 4. The tensile strength of the scaffold S1, S2 and S3 are 0.77, 0.8 and 0.66 MPa respectively. The tensile strength of scaffold S3 is decreased from 0.77 to 0.66 MPa due the increased POCS content in FBN. From the figure 4, the elongation break point for the scaffold S3 occurring at 67%, which is between scaffold S1 and S2 are 45% and 96% respectively. The literature reported elongation break point is about 60 % [29]. Consequently, the Young's modulus of scaffold S3 is about 0.27 ± 0.07 MPais very low compared to the 0.46 ± 0.21 and 0.43 ± 0.08 MPais for S1 and S2. Hence, scaffold S3 is more elastic than the rest. The tensile strength and young's modulus of the different elastomers are presented in table-2, in comparison with POCS/FBN of the current study. scaffold elasticity influence the adherence between neighbouring cells to promote tissue formation, where bio-elastomeric scaffolds stimulate supporting contacts [30]. The scaffold S3 indicates the satisfactory elasticity requirement for the cardiac scaffolds. Cell-scaffold construct interactions resembling the native micro-environment with appropriate structural and chemical cues are aimed in tissue engineering[16].

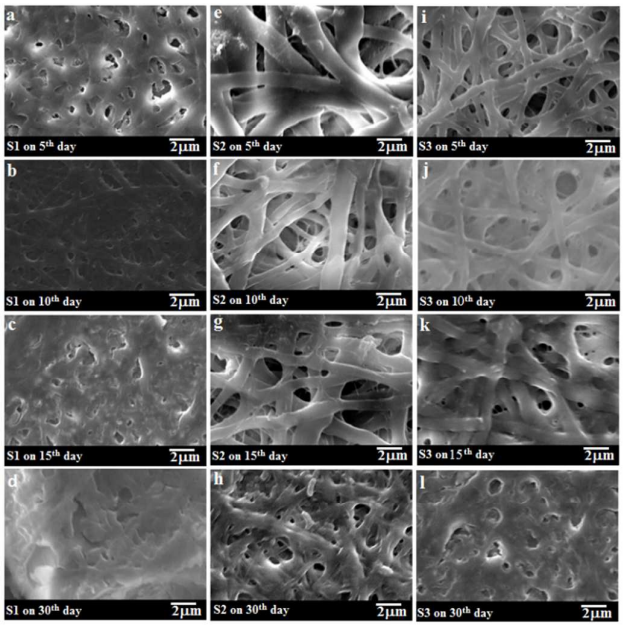

Figure 2: SEM morphology of S1 (a, b, c and d), S2 (e, f, g and h) and S3 (i, j, k and l) for 5, 10, 15 and 30 days respectively.

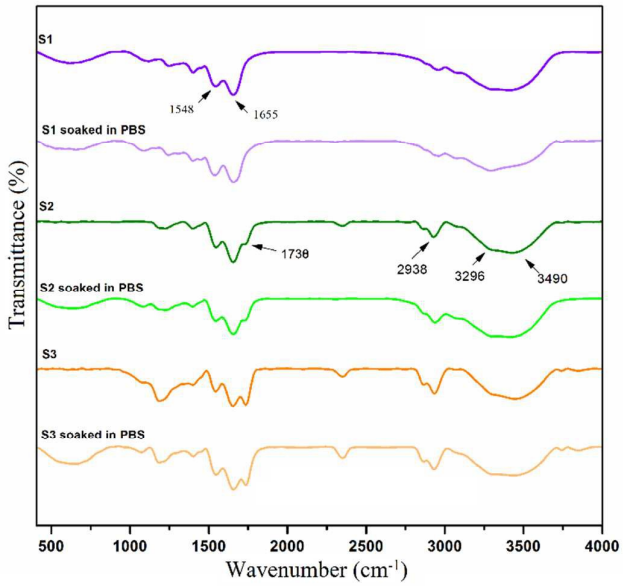

Figure 3: FTIR spectral analysisof scaffold S1, S2 and S3 before and after PBS soaking.

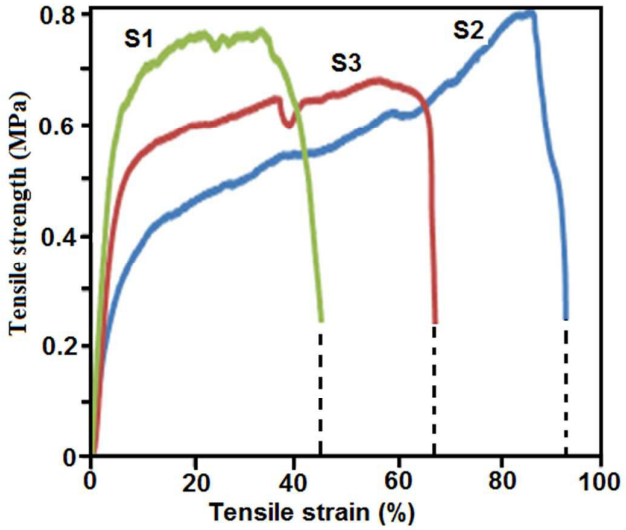

Figure 4: Tensile stress–strain curves of electrospun scaffolds (a) S1 (b) S2 and (c) S3.

Table 1: Experimental properties of scaffolds S1, S2 and S3.

scaffold	POCS:FBN	a (°)	b (nm)	c	d	e
S1	0:100	111.65 ± 8	400 ± 180	0.77	0.46 ± 0.21	5th
S2	25:75	48.81 ± 9	560 ± 110	0.80	0.43 ± 0.08	30thpartly
S3	50:50	58.85 ± 10	440 ± 120	0.66	0.27 ± 0.07	15thstarted, 30thday complete

*a: Contact angle in degrees; b: Diameters in nm; c: Tensile Strength in MPa;d: Young's modulus in MPa and e: Degradation studies in days.

Table-2: The tensile properties of elastomers, reproduced with copyright permission from Ref[31]

Synthetic polymers		A	B	Ref.
PU	scaffold	2-60	11-1690	[8]
PGS	scaffold	0.5	0.04-0.282	[31]
POC	scaffold	6.7	1-16	[31]
POCS	scaffold S3	0.66	0.27	Present study
PHB	scaffold	36	2000-3000	[32]
PPD(=PDS)	scaffold	12	600	[32]
PLLA or PDLLA	scaffold	30-80	1000-4000	[32]
TMC	scaffold	12	6	[33]
TMC/PDLLA	scaffold	10	16	[33]
PGA	scaffold	70	7000-10000	[32]

A: Tensile Strength in MPa; B: Young's modulus in MPa. PU: Polyurethane, PGS: Polyglycerol sebacate, POC: poly [1,8-octanediol-co-(citric acid); PHB: Poly(3 or 4-hydroxybutyrate);PPD(=PDS): Poly (p-dioxanone);PLLA: Poly(L-lactic acid); PDLLA: Poly(D,L-lactic acid); TMC: Poly (1,3-trimethylene carbonate); PGA: Poly(glycolic acid).

3.1. Biocompatibility of Scaffolds:

The cell propagation performance was tested on the scaffolds of TCP, S1, S2 and S3 and presented in figure 5. The MTS assay results confirms the nontoxicity of scaffolds. The scaffold S3 was found to show high propagation number of cells and this could be due to the elasticity and topography of the scaffolds S3. In addition, cell proliferation performance for the scaffold S3 is found to increase 23 % to 57.85 %. The biocompatibility was examined by using HCMs followed for the six days of cell culture and presented in figure 6. The relative cellular proliferation of HCMs was found higher on scaffold S3 than on scaffold S1, S2 and TCP. For the scaffold S3 the rate of cell proliferation was prominent on composite scaffold S3 on day six when compared to the TCP, S1 and S2 scaffolds. The structure of composite scaffold S3 facilitated the elasticity that might enhanced the proliferation. By mimicking the native ECM architecture and anisotropic flexibility of composite scaffold S3 would provide the extensive cellular growth.

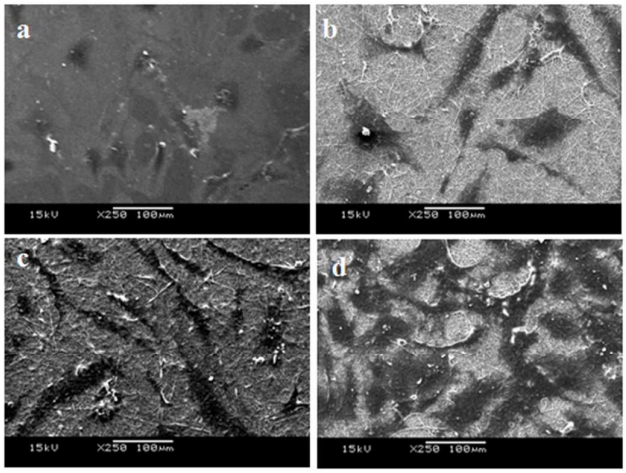

Figure 5: SEM images of Human cardiomyocytes on (a)TCP(b) S1 (c) S2 and (d) S3.

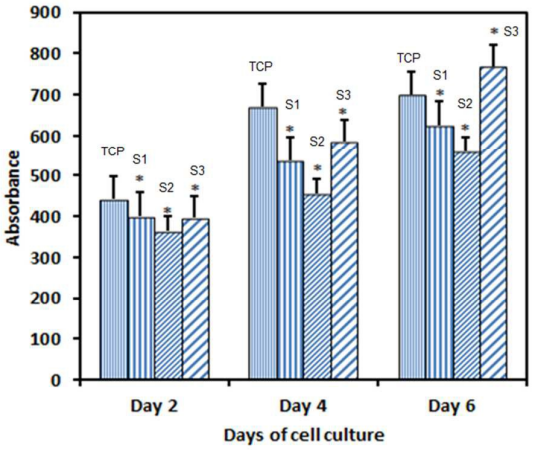

Figure 6: Cell proliferation study of cardiomyocytes on Day 2, 4 and 6 by MTS. *Significant difference against cell proliferation on TCP, S1, S2 and S3 scaffolds with FBN at p≤0.05.

The cell morphology on scaffold S3 revealed that the nano dimensions of scaffold favours the HCMs to grow a great extent. The cell morphology of the composite scaffolds are similar to its appearance in the native human heart and might be an advantage in correlating the contractile behaviour of cardiomyoctyes[34]. Cell-to-cell interaction was observed and found that the scaffold S3 is predominant when compared to TCP, S1 and S2. The composite scaffold S3 exhibited homogeneous distribution compared to other substrates and this might be due to mechanical cues provided by the scaffold.

3.2. Immunofluorescence of Scaffolds:

Cardiac Troponin-I and MHCs are most important in cardiac muscle tissue and functioning[35, 36]. The expression of Troponin-I and MHCs are presented in figure-7 and figure 8 respectively. From the figure 7, Scaffold S3 confirms the expression is perfect when compared to TCP and FBN scaffolds due to the softness which came from the composites. In addition, scaffold S3 is mechanically more elastic than rest, we presume that the more prominent expression of marker proteins presented in case of scaffold S3. From the figure 8, the expression of MHC was dominant on scaffold S3 compared to remaining scaffolds. The fabrication of a scaffold resembling the natural environment with comparable mechanical properties specifically elasticity could favour the cell adhesion and proliferation. The results of the immunofluorescent studies suggested the functionality of cells seeded on the scaffold S3 and could be potential scaffold for cardiac tissue regeneration.

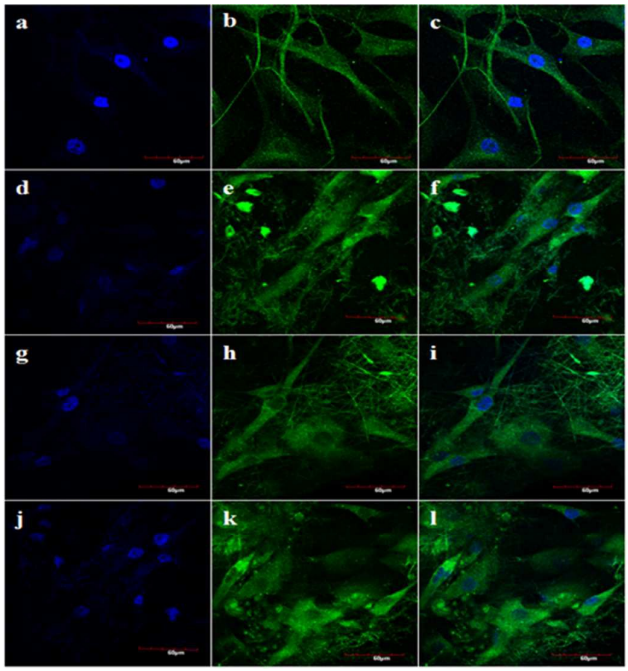

Figure 7: The cardiac specific protein expression of Trp-I on TCP, S1, S2 and S3 on day 4. Where (a, d, g, j) images are cell nuclei stained DAPI; the images (b, e, h, k) shown after staining with Alexaflour 488 and the merged images are shown in (c, f, i, l).

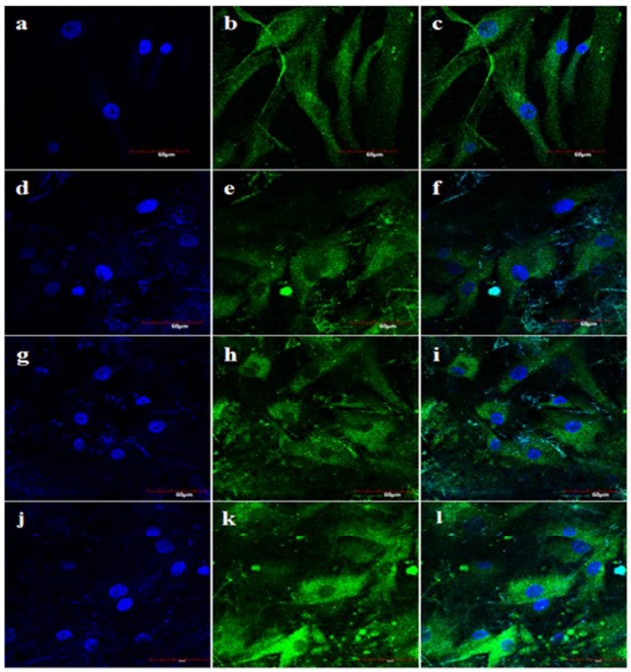

Figure 8: The cardiac specific protein expression of MHC on TCP, S1, S2 and S3 on day 4. Where (a,d,g,j) images are cell nuclei stained DAPI; the images (b,e,h,k) shown after staining with Alexaflour 488 and the merged images are shown in (c,f,i,l).

Cardiac protein, Trp-I has a molecular weight of 37,000 Da[37]. During the cardiomyocyte damage, the loss of membrane integrity causes the release of cardiac troponins into the blood circulation but in the Apoptosis (programmed cell death) does not affects in deficit of cell membrane and do not release the troponins [38] and play a role in establishing prognosis of myocardial infarction (MI) any troponin levels increases above the normal levels is cohort with an increased risk of adverse events[39]. The mechano-enzyme myosin is the crucial protein, and contains the typical cardiac myofibrillar protein [40]. The protein expression Trp-I and MHC of the cardiomyocytes on the electrospun nanofibrous scaffolds were analysed by immunostaining analysis. As shown in Figures 7 and 8, cardiomyocytes on nanofibers expressed higher levels of Trp-I and MHC respectively on composite scaffold S3 provides cues for contractile ability and functionality of cardiomyocytes compared than TCP, S1 and S2. The results of the immunofluorescent studies suggested the functionality of cells seeded on the electrospun scaffold S3 and could be potential scaffold for cardiac tissue regeneration. The biocompatibility studies on POCS/FBN using cardiac myocytes encountered as toxic free, through which scaffold S3 show excellent cell growth than the S1 and S2. Our studies manifest the possibility of electrospinning POCS/FBN containing elastomeric scaffold, as applicable bio-scaffold for cardiac tissue engineering.

4. Conclusions:

A mixture of elastomeric polymer POCS and FBN composite electrospun nanofibrous scaffolds were successfully

synthesized. These composite scaffolds were characterized and carried further bio experimental investigations. The water contact angle was observed in the range of the 40 – 70 ° which is reasonable for cell adhesion. The scaffold diameters were obtained from SEM images and were in the range of cell growth requirement. The FT-IR peak was observed at 1738 cm^{-1} which confirms the elastomer and after the PBS treatment no change in peak position was observed. From the tensile test measurements the Young's modulus was in comparable to those with native human myocardium (HMC). On further the scaffolds were carried for cell proliferation by means of MTS assay. HCMs were seeded on the scaffolds and the interaction of cell-scaffold constructs were evaluated in this study. Proliferation of CMs on scaffold S3 was observed to increase from day two to six. The interactions between cells and substrate were analysed by using confocal microscopy. The electrospun composite scaffolds of POCS/FBN proved to yield flexibility and degradation. In-vitro compatibility testing of POCS with HCMs proved that the scaffold S3 is an outstanding elastomeric scaffold which would anticipate to be implanted for potential MI regeneration.

Acknowledgements:

This study was supported by the NRF-Technion (R-398-001-065-592), and NUSNNI, National University of Singapore, Singapore. MS thanked Prof. A S Nair, Amrita Centre for Nanosciences and Molecular Medicine, Amrita University, Kochi, India for synthesizing POCS polymer. MS thanking Dr. M. P. Prabhakaran, NUSCNN, National University of Singapore, Singapore for helping all experimental analysis.

5. References:

1. R. Langer and J. P. Vacanti, *Science*, 1993, **260**, 920-926.
2. W. H. Zimmermann, I. Melnychenko and T. Eschenhagen, *Biomaterials*, 2004, **25**, 1639-1647.
3. K. L. Christman and R. J. Lee, *J. Am. Coll. Cardiol*, 2006, **48**, 907-913.
4. F. Caiado, T. Carvalho, F. Silva, C. Castro, N. Clode, J. F. Dye and S. Dias, *Biomaterials*, 2011, **32**, 7096–7105.
5. D. Wiedemann, S. Schneeberger, P. Friedl, K. Zacharowski, N. Wick, F. Boesch, R. Margreiter, G. Laufer, P. Petzelbauer and S. Semsroth, *Transplantation*, 2010, **89**, 824–829.
6. M. C. Barsotti, F. Felice, A. Balbarini and R. D. Stefano, *Biotechnol. Appl. Biochem.*, 2011, **58**, 301–310.
7. Y. Wang, G. A. Ameer, B. J. Sheppard and R. Langer, *Nat. Biotechnol.*, 2002, **20**, 602-606.
8. Q. Chen, S. Liang and G. A. Thouas, *Prog. Polym. Sci.*, 2012, **38**, 584-671.
9. I. Djordjevic, N. R. Choudhury, N. K. Dutta and S. Kumar, *Polym.Iner.*, 2011, **60**, 333-343.
10. I. Djordjevic, N. R. Choudhury, N. K. Dutta and S. Kumar, *Polymer*, 2009, **50**, 1682-1691.
11. L. Niklason, J. Gao, W. Abbott, K. K. Hirschi, S. Houser, R. Marini and R. Langer, *science*, 1999, **284**, 489-493.
12. L. Niklason, W. Abbitt and J. Gao, *J. Vasc. surg.*, 2001, **33**, 628-638.
13. J. Yang, A. R. Webb and G. A. Ameer, *Adv.Mater.*, 2004, **16**, 511-516.
14. M. P. Crapo and Y. Wang, *Biomaterials*, 2010, **31**, 1626-1635.
15. V. J. Babu, S. Vempati, T. Uyar and S. Ramakrishna, *Physical Chemistry Chemical Physics*, 2015, **17**, 2960-2986.
16. M. P. Prabhakaran, A. S. Nair, D. Kai and S. Ramakrishna, *Biopolymers*, 2012, **97**, 529-538.
17. M. M. Stevens and J. H. George, *Science*, 2005, **310**, 1135-1138.
18. S. A. Sell, P. S. Wolfe, K. Garg, J. M. McCool, I. A. Rodriguez and G. L. Bowlin, *Polymers*, 2010, **2**, 522-553.
19. M. C. McManus, E. D. Boland, H. P. Koo, C. P. Barnes, K. J. Pawlowski, G. E. Wnek, D. G. Simpson and G. L. Bowlin, *Acta Biomater.*, 2006, **2**, 19-28.
20. C. He, X. Xu, F. Zhang, L. C. Feng, H. Wang and X. Mo, *J. Biomed. Mater. Res. A*, 2001, **97A**, 339–347.
21. E. Dejane, S. Collela, L. Languino, G. Balconi, G. C. GC and P. Marchisio, *J Cell Biol*, 1987, **104**, 1403-1411.
22. A. J. Bretland, J. Lawry and R. M. Sharrard, *Cell Proliferat*, 2001, **34**, 199–210.
23. I. Djordjevic, N. R. Choudhury, N. K. Dutta, S. Kumar, E. J. Szili and D. A. Steele, *J. Biomater. Scie*, 2010, **21**, 237-251.
24. V. J. Babu, K. K. Satheesh, D. C. Trivedi, V. R. K. Murthy and T. S. Natarajan, *J.Eng.Fiber Fabr.*, 2007, **2**, 25-31.
25. V. J. Babu, R. S. R. Bhavatharini and S. Ramakrishna, *RSC Adv.*, 2014, **4**, 19251-19256.
26. Y. Arima and H. Iwata, *Biomaterials*, 2007, **28**, 3074-3082.
27. S. Sell, C. Barnes, D. Simpson and G. Bowlin, *J. Biomed. Mater. Res. A*, 2008, **85**, 115-126.
28. M. Chen, P. K. Patra, S. B. Warner and S. Bhowmick, *Tissue Eng.* , 2007, **13**, 579.
29. M. M. Aygen and E. Braunwald, *Circulation*, 1962, **26**, 516-524.
30. C. Reinhart-King, M. Dembo and D. Hammer, *Biophys J.*, 2008, **95**, 6044–6051.
31. Q.-Z. Chen, S. E. Harding, N. N. Ali, A. R. Lyon and A. R. Boccaccini, *Mater. Sci. Eng. R*, 2008, **59**, 1-37.
32. A. R. Webb, J. Yang and G. A. Ameer, *Expert Opin.Biol.Ther.*, 2004, **4**, 801-812.
33. A. P. Pego, A. A. Poot, D. W. Grijpma and J. Feijen, *J.Control Release*, 2003, **87**, 69-79.
34. D. N. Rockwood, Robert E Akins Jr., I. C. Parrag, K. A. Woodhouse and J. F. Rabolt, *Biomaterials*, 2008, **29**, 4783–4791.
35. M. Yang, S. Wang, N. Chi, Y. Huang, LChang, M. Shieh and T. Chung, *Biomaterials*, 2009, **30**, 3757–3765.
36. K. Nakao, W. Minobe, R. Roden, R. M. Bristow and A. L. Leinwand, *J. Clin. Invest.*, 1997, **100**, 2362–2370.
37. B. Goldmann, R. Christenson and C. H. etal, *Curr. Control Trials Cardiovasc. Med.* , 2001, **2**, 75-84.
38. S. Kostin, L. Pool, A. Elsasser and etal, *Circ Res* 2003, **92**, 715–724.
39. C. W. Hamm, B. U. Goldmann and C. Heeschen, *New Engl J Med*, 1997, **337**, 1648–1653.
40. M. A. Geeves and K. C. Holmes, *Annu. Rev. Biochem*, 1999, **68**, 687-728.

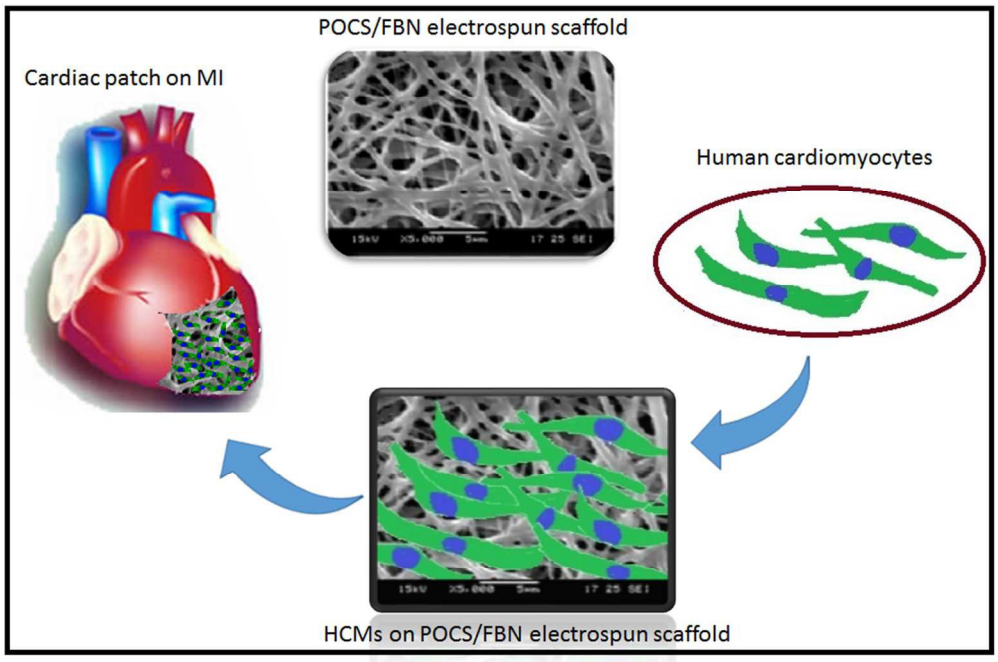

A schematic representation for nanofiber with HCMs in cardiac tissue engineering
258x170mm (96 x 96 DPI)